# Solubilization of Membrane Proteins into Functional Lipid-Bilayer Nanodiscs Using a Diisobutylene/Maleic Acid Copolymer

Abraham Olusegun Oluwole, Bartholomäus Danielczak, Annette Meister,
Jonathan Oyebamiji Babalola, Carolyn Vargas, and Sandro Keller*

Abstract: *Once removed from their natural environment, membrane proteins depend on membrane-mimetic systems to retain their native structures and functions. To this end, lipid-bilayer nanodiscs that are bounded by scaffold proteins or amphiphilic polymers such as styrene/maleic acid (SMA) copolymers have been introduced as alternatives to detergent micelles and liposomes for in vitro membrane-protein research. Herein, we show that an alternating diisobutylene/maleic acid (DIBMA) copolymer shows equal performance to SMA in solubilizing phospholipids, stabilizes an integral membrane enzyme in functional bilayer nanodiscs, and extracts proteins of various sizes directly from cellular membranes. Unlike aromatic SMA, aliphatic DIBMA has only a mild effect on lipid acyl-chain order, does not interfere with optical spectroscopy in the far-UV range, and does not precipitate in the presence of low millimolar concentrations of divalent cations.*

Integral membrane proteins perform a plethora of cellular functions and are major drug targets.[1] Their extraction, purification, and in vitro investigation often remain challenging[2] because the hydrophobic transmembrane segments of these proteins dictate the use of amphiphilic compounds that form membrane-mimetic nanoenvironments to confer solubility in aqueous media. Detergents are traditionally used for solubilization,[2] although their micellar assemblies do not adequately reproduce some of the hallmarks of the native lipid-bilayer environment. Detergent-purified proteins can be reconstituted into liposomes; however, the large size of liposomes is incompatible with many chromatographic and

optical spectroscopic techniques as well as solution NMR spectroscopy. The advent of nanodiscs assembled from phospholipids and membrane-scaffold proteins (MSPs) marked substantial progress in the development of nanosized lipid-bilayer particles.[3] More recently, styrene/maleic acid (SMA) copolymers (Figure 1a) have been found to recruit
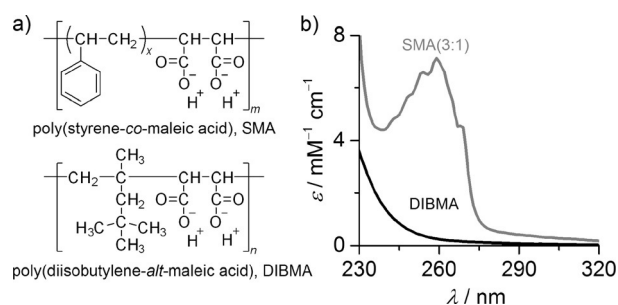
Figure 1. a) Chemical structures of SMA(3:1) (number average $m \approx 9$, $x \approx 3$, $M_n = 4.0 \text{ kg mol}^{-1}$) and DIBMA (number average $n \approx 37$, $M_n = 8.4 \text{ kg mol}^{-1}$). b) Molar extinction coefficients ε of SMA(3:1) and DIBMA as functions of wavelength λ.

membrane proteins and associated lipids directly from natural or artificial membranes into "native nanodiscs" or SMA/lipid particles (SMALPs).[4–13] Hence, without requiring assistance from conventional detergents, SMA solubilizes and stabilizes a variety of membrane proteins, ranging from bacteriorhodopsin[4,5] to ABC transporters,[4,7] ion channels,[6] bacterial reaction centers,[8] and G-protein-coupled receptors.[9,12]

Unfortunately, optical spectroscopic studies on membrane proteins embedded in either MSP nanodiscs or SMALPs are hampered by the strong UV absorption of the disc scaffold, that is, MSP or SMA, respectively (Figure 1b). Thus, although the direct extraction of membrane proteins into SMALPs presents a number of advantages[10,11,13] over detergent-based approaches,[2] the amount of protein solubilized by SMA cannot be readily quantified using UV absorbance.[6,11] For the same reason, far-UV circular dichroism (CD) spectra of proteins in SMALPs can be acquired only after the removal of protein-free nanodiscs,[4,6,7,9,12] and the presence of phenyl moieties can pose problems during purification steps involving column materials prone to nonspecific interactions with aromatic groups.[10,11,13] Moreover, SMA precipitates in the presence of low concentrations of divalent cations, which renders it incompatible with many biochemical or functional protein assays that depend on Mg^{2+} or Ca^{2+}.[10,11,13] Herein, we address these challenges by demonstrating that a diisobutylene/maleic acid (DIBMA) copolymer (Figure 1a) efficiently

[*] A. O. Oluwole, B. Danielczak, Dr. C. Vargas, Prof. Dr. S. Keller
Molecular Biophysics, University of Kaiserslautern
Erwin-Schrödinger-Str. 13, 67663 Kaiserslautern (Germany)
E-mail: mail@sandrokeller.com

A. O. Oluwole, Prof. Dr. J. O. Babalola
Department of Chemistry, University of Ibadan
200284, Ibadan (Nigeria)

Priv.-Doz. Dr. A. Meister
Institute of Chemistry and Institute of Biochemistry
and Biotechnology, Martin Luther University Halle-Wittenberg
Von-Danckelmann-Platz 4, 06120 Halle (Germany)

Supporting information and the ORCID identification number(s) for the author(s) of this article can be found under http://dx.doi.org/10.1002/anie.201610778.

solubilizes lipids and proteins to generate nanodiscs harboring a natively folded and functionally active integral membrane enzyme that is directly amenable to UV spectroscopy as well as a Ca²⁺-dependent enzyme activity assay. Our finding that DIBMA is able to extract proteins of largely different sizes from native membranes indicates that this novel solubilizing polymer is applicable to a broad range of target proteins.

DIBMA is an alternating copolymer of maleic acid and diisobutylene (2,4,4-trimethylpent-1-ene) that is commercially available under the trade name Sokalan CP9 (BASF, Germany) with a nominal molar mass of 12 kg mol⁻¹. Buffered DIBMA solutions can readily be prepared from stock solutions through dialysis without laborious precipitation, washing, and lyophilization steps.[11,13] After dialysis, size-exclusion chromatography (SEC) coupled to refractive-index and light-scattering detection yielded a mass-average molar mass of $M_w = 15.3$ kg mol⁻¹, a number-average molar mass of $M_n = 8.4$ kg mol⁻¹, and thus a dispersity of $M_w/M_n = 1.82$ (Figure S1 in the Supporting Information). As anticipated, we found the far-UV extinction coefficient of aliphatic DIBMA to be much lower than that of aromatic SMA (Figure 1b). We examined the membrane-solubilizing capacity of DIBMA and the emergence of DIBMA/lipid particles (DIBMALPs) by exposing large unilamellar vesicles (LUVs) made of the phospholipid 1,2-dimyristoyl-sn-glycero-3-phosphocholine (DMPC) to increasing polymer concentrations and monitoring nanoparticle formation by dynamic light scattering (DLS), transmission electron microscopy (TEM), and ³¹P NMR spectroscopy.

Upon addition of DIBMA, the turbidity typical of DMPC LUVs cleared within a few seconds (Figure S2a). Particle size distributions derived from DLS (Figure 2a, Figure S2b–d) revealed an increase in apparent hydrodynamic diameter from around 150 nm to more than 1000 nm before solubilization set in. Thereafter, the hydrodynamic diameter smoothly decreased to approximately 35 nm at a DIBMA/DMPC molar ratio of 0.08 and further to approximately 18 nm at a ratio of 0.20 (Figure 2b). Hence, DIBMALPs are somewhat larger than SMALPs, which under comparable conditions have diameters of around 29 nm and 13 nm, respectively.[14] DIBMA also proved effective in solubilizing longer-chain phospholipids such as 1,2-dipalmitoyl-sn-glycero-3-phosphocholine (DPPC; Figure S3) and shorter-chain variants such as 1,2-dilauroyl-sn-glycero-3-phosphocholine (DLPC; see Figure 4). Negative-stain TEM showed DIBMALPs to be homogeneous disc-shaped particles (Figure 2c).

In ³¹P NMR experiments, the signal of slow-tumbling DMPC LUVs was broadened beyond detection, but an isotropic peak emerged upon addition of DIBMA (Figure 2d), the intensity of which reflected the amount of solubilized lipid.[14,15] The peak areas at each DMPC concentration revealed two breakpoints marking the onset (SAT) and completion (SOL) of solubilization (Figure 2e). Plotting the DIBMA concentrations at the SAT and SOL boundaries against the corresponding DMPC concentrations yielded a phase diagram (Figure 2f) characterized by saturating and solubilizing DIBMA/DMPC molar ratios of $R_S^{b,SAT} = 0.030 \pm 0.005$ and $R_S^{m,SOL} = 0.062 \pm 0.004$, with vanishing ordinate
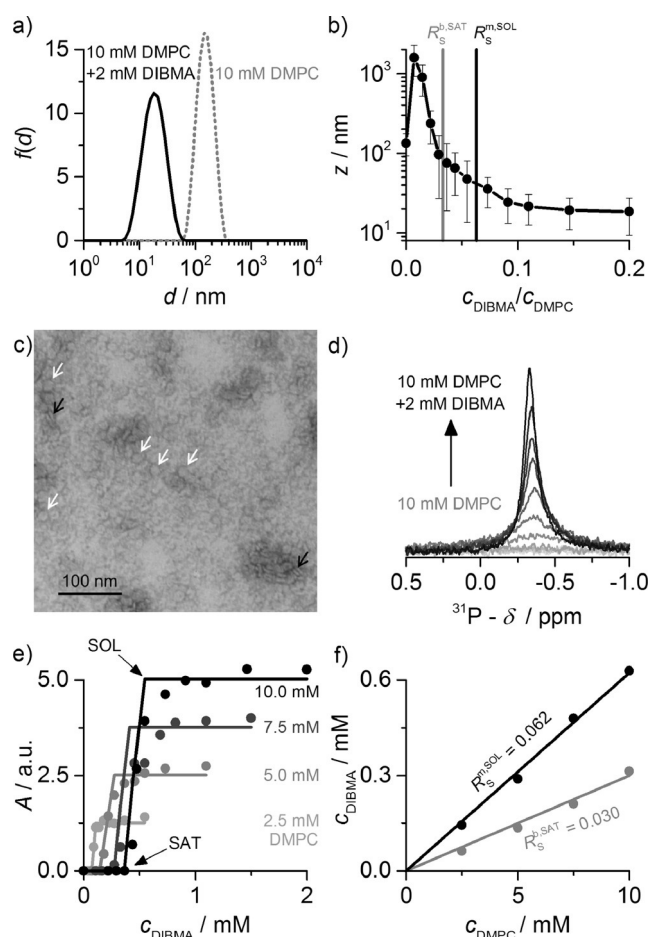
Figure 2. Solubilization of lipid vesicles by DIBMA at 30°C. a) Intensity-weighted distributions $f(d)$ of the hydrodynamic particle diameter d before and after addition of DIBMA to DMPC LUVs. b) z-Average hydrodynamic diameter z of 10 mM DMPC titrated with DIBMA. Vertical bars are size-distribution widths calculated from polydispersity indices. Vertical lines indicate saturation and solubilization thresholds from NMR data [see (f)]. c) TEM image of DIBMALPs ($c_{DIBMA}/c_{DMPC} = 0.10$). White and black arrows indicate discs in face-on and edge-on views, respectively. d) ³¹P NMR spectra of DMPC titrated with DIBMA. e) NMR peak areas A at four DMPC concentrations as functions of DIBMA concentration. Lines are fits according to Equations (S11)–(S13) in the Supporting Information. f) DMPC/DIBMA phase diagram with saturation and solubilization boundaries obtained from (e).

intercepts suggesting a negligible concentration of "free" polymer. From these molar ratios, we derived free-energy changes accompanying the transfer of DMPC and DIBMA from vesicles into DIBMALPs of $\Delta G_L^{b \to m,o} = (0.077 \pm 0.010)$ kJ mol⁻¹ and $\Delta G_S^{b \to m,o} = -(1.76 \pm 0.09)$ kJ mol⁻¹, respectively. Under similar conditions, DMPC solubilization by SMA(3:1) is described by critical molar ratios of $R_S^{b,SAT} = 0.078 \pm 0.008$ and $R_S^{m,SOL} = 0.144 \pm 0.014$, which correspond to vesicle-to-SMALP transfer free energies of $\Delta G_L^{b \to m,o} = (0.15 \pm 0.05)$ kJ mol⁻¹ and $\Delta G_S^{b \to m,o} = -(1.36 \pm 0.45)$ kJ mol⁻¹.[14] Such marginal free-energy penalties incurred upon lipid transfer from vesicular bilayers into both kinds of nanodiscs attest to the gentle nature of lipid solubilization by DIBMA and SMA(3:1).

We compared the effects of DIBMA and SMA(3:1) on the conformational order of phospholipid acyl chains by Raman spectroscopy. Importantly, there were no major differences in the vibrational frequencies or intensities of representative DMPC bands before and after solubilization by DIBMA, either in the gel phase at 10°C (Figure 3a) or in
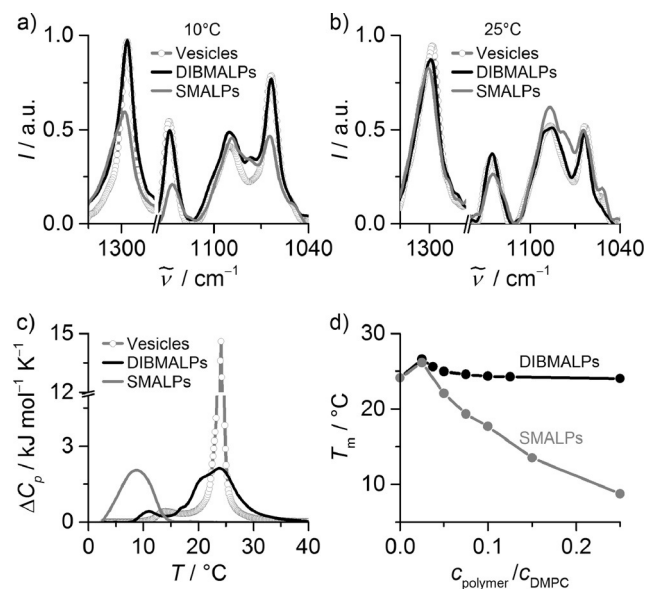
Figure 3. Influence of polymers on lipid acyl-chain order and phase behavior. a,b) Raman spectra giving relative intensities I as functions of wavenumber $\tilde{\nu}$ for 10 mM DMPC in LUVs, DIBMALPs ($c_{DIBMA}/c_{DMPC}=0.35$), and SMALPs ($c_{SMA}/c_{DMPC}=0.40$) at 10°C (a) and 25°C (b). c) DSC thermograms showing excess molar isobaric heat capacities ΔC_p of 5 mM DMPC in LUVs, DIBMALPs ($c_{DIBMA}/c_{DMPC}=0.20$), and SMALPs ($c_{SMA}/c_{DMPC}=0.25$). d) Melting temperature T_m of 5 mM DMPC in DIBMALPs and SMALPs versus polymer/lipid ratio.

the fluid state at 25°C (Figure 3b). By contrast, solubilization by SMA(3:1) resulted in significant shifts and intensity reductions in the C−C stretching bands near 1125 cm^{-1} and 1060 cm^{-1} as well as the methylene twisting mode near 1300 cm^{-1}, particularly at 10°C (Figure 3a) but also at 25°C (Figure 3b). These observations are ascribed to a loss in acyl-chain order as the number of *gauche* defects increases[16,17] upon SMALP formation, whereas vesicle-like chain order is preserved in DIBMALPs in both phase states of DMPC.

We further compared the distinct effects of the two polymers by monitoring the thermotropic phase transition of DMPC with the aid of differential scanning calorimetry (DSC). DMPC LUVs gave rise to a sharp gel-to-fluid transition at 24°C. Upon solubilization by DIBMA or SMA-(3:1), the transition became broader (Figure 3c, Figure S4a,b), thus indicating the existence of bilayer structures of smaller size.[18,19] The calorimetric enthalpy decreased from 1.5 kJ mol^{-1} in LUVs to 1.0 kJ mol^{-1} and 0.84 kJ mol^{-1} in DIBMALPs and SMALPs, respectively, while the van't Hoff enthalpy was reduced from approximately 94 kJ mol^{-1} to approximately 15 kJ mol^{-1} in both cases. Thus, the "cooperative unit", taken as the ratio of the van't Hoff enthalpy to the

calorimetric enthalpy, diminished from more than 60 lipid molecules in LUVs to fewer than 25 lipids in both types of nanodiscs (Figure S4c). While the reduced cooperativity reflects the nanoscale size of DIBMALPs and SMALPs, the decrease in calorimetric enthalpy must result from a fraction of DMPC being in contact with the polymer scaffolds along the rim of the nanodiscs. In sharp contrast with the situation encountered in SMALPs, the transition temperature was not downshifted upon solubilization by moderate DIBMA concentrations (Figure 3d). This suggests much less perturbation of lipid packing by DIBMA compared with SMA(3:1), the stronger effect of which is thought to result from intrusion of its phenyl rings into the bilayer core.[19,20] With DIBMALPs, similarly low transition temperatures of around 10°C were reached only at much higher polymer/lipid ratios (Figure S4d). The gentle solubilizing properties of the branched aliphatic side chain of DIBMA may have important implications for stabilizing and studying membrane proteins with functions that depend on lipid order and dynamics.[21]

The ability of DIBMA to solubilize an integral membrane protein was tested on DLPC proteoliposomes containing outer membrane phospholipase A (OmpLA)[22] and, for comparison, protein-free DLPC liposomes. Solubilization of the proteoliposomes yielded sharp ^{31}P NMR peaks (Figure 4a) and was as efficient as in the absence of protein (Figure 4b). At a DIBMA/DLPC molar ratio of 0.20, both protein-free and OmpLA-loaded DIBMALPs were found to be disc-shaped particles with diameters of approximately 15 nm (Figure 4c–e). Crucially, OmpLA fully retained its enzymatic activity in DIBMALPs (Figure 4f), which remained in suspension without any signs of aggregation or precipitation upon Ca^{2+}-mediated phospholipase activation. Of note, enzyme assays of OmpLA in SMALPs failed because the latter precipitated with as little as 2 mM Ca^{2+} (Figure S5a), whereas DIBMALPs were found to tolerate at least 20 mM Ca^{2+} (Figure S5b) or Mg^{2+} (Figure S6).

The absence of UV-absorbing groups in DIBMA allowed us to utilize CD spectroscopy to assess the secondary structure and stability of OmpLA in DIBMALPs without the prior removal of protein-free nanodiscs. Folded OmpLA exhibited a CD maximum at 232 nm and a pronounced minimum at 218 nm, which are typical of high β-strand content.[22] In DIBMALPs, OmpLA retained these spectral characteristics even in the presence of high urea concentrations (Figure 4g) and at elevated temperatures (Figure S7a), thus demonstrating that DIBMALPs impart considerable conformational stability to the protein, as has been shown for OmpLA in vesicular lipid bilayers.[23] By contrast, no CD spectra could be obtained from OmpLA in unpurified SMALPs (Figure S7b) because of the prohibitively strong UV absorption of the SMA scaffold. This agrees with earlier reports[4,6,7,9,12] that proteins in SMALPs are amenable to UV spectroscopy only after the removal of protein-free nanodiscs. Although the latter can be achieved by chromatographic purification,[11,13] there are considerable advantages to extracting membrane proteins into an environment that immediately enables reliable concentration determination by UV absorbance as well as deeper scrutiny by optical spectroscopic techniques such as far-UV CD[24] prior to any
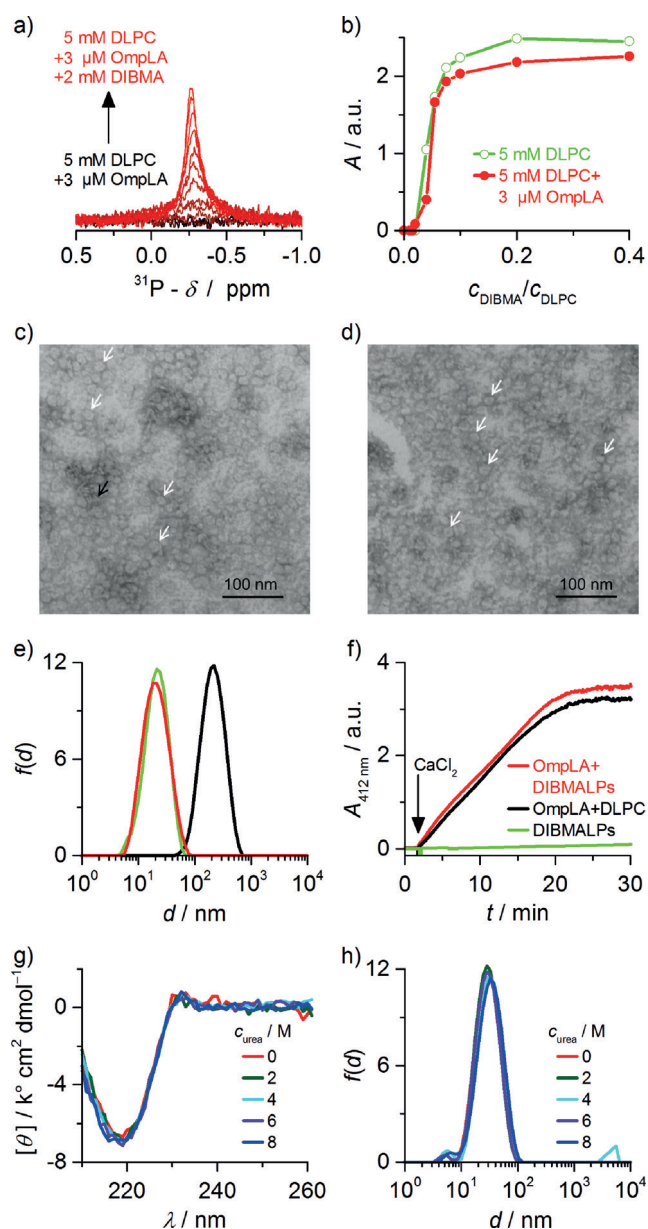
Figure 4. Solubilization, activity, and stability of OmpLA in DIBMALPs at 20°C. a) ^{31}P NMR spectra of DLPC harboring OmpLA upon titration with DIBMA. b) NMR peak areas A of DLPC in the presence or absence of OmpLA upon titration with DIBMA. c) TEM image of DIBMALPs without protein ($c_{DIBMA}/c_{DLPC} = 0.20$). d) TEM image of OmpLA-containing DIBMALPs ($c_{DLPC}/c_{OmpLA} \approx 1800$). White and black arrows indicate discs in face-on and edge-on views, respectively. e) Intensity-weighted particle size distributions $f(d)$ of proteoliposomes (5 mM DLPC, 3 µM OmpLA; black), protein-free DIBMALPs (5 mM DLPC, 1 mM DIBMA; green), and OmpLA-containing DIBMALPs (5 mM DLPC, 3 µM OmpLA, 1 mM DIBMA; red). f) UV absorbance at 412 nm ($A_{412 nm}$) as a function of time t for monitoring the phospholipase kinetics of 0.3 µM OmpLA in proteoliposomes (0.5 mM DLPC) and DIBMALPs (0.5 mM DLPC, 0.1 mM DIBMA); no activity was observed with protein-free DIBMALPs. g,h) Far-UV CD spectra showing mean molar residual ellipticities $[\theta]$ as functions of wavelength λ (g) and $f(d)$ (h) as measured for 3 µM OmpLA in DIBMALPs (5 mM DLPC, 1 mM DIBMA) in the presence of increasing urea concentrations.

further treatment. Furthermore, the small particle size and narrow size distribution of DIBMALPs were maintained even under strongly denaturing conditions (Figure 4 h), which contrasts with the drastic effects of chaotropes on the size and morphology of detergent micelles[25] and MSP nanodiscs.[26]

To demonstrate the compatibility of DIBMALPs with protein-chromatographic methods, we subjected samples produced by solubilizing proteoliposomes with various DIBMA concentrations to SEC. Elution profiles revealed a first peak corresponding to DIBMALPs that contained OmpLA and a second peak reflecting protein-free nanodiscs (Figure 5a). After SEC purification, OmpLA-containing
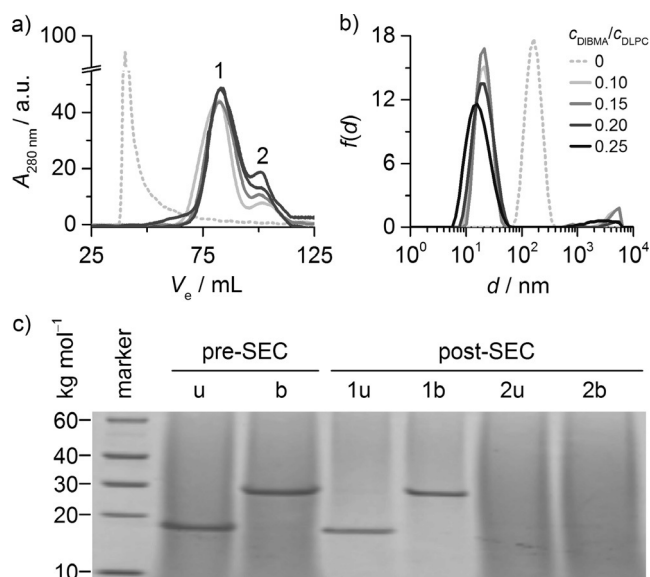
Figure 5. Chromatographic separation of OmpLA-containing DIBMALPs at 8°C. a) SEC profiles as monitored by UV absorbance at 280 nm ($A_{280 nm}$) versus elution volume V_e (20 mM DLPC, 13 µM OmpLA, 0–5 mM DIBMA). b) Intensity-weighted particle size distributions $f(d)$ of proteoliposomes and OmpLA-containing DIBMALPs at various c_{DIBMA}/c_{DLPC} after SEC. Samples correspond to pooled fractions in peak 1 eluting at $V_e \approx 85$ mL in (a). c) SDS-PAGE showing that OmpLA was present and natively folded in DIBMALPs ($c_{DIBMA}/c_{DLPC} = 0.20$) before and after SEC in peak 1 but absent from peak 2. u = unboiled; b = boiled.

DIBMALPs appeared as homogeneously sized particles with a diameter of approximately 20 nm at a DIBMA/DLPC molar ratio of 0.10, which further diminished to around 12 nm at a ratio of 0.25 (Figure 5b). OmpLA remained natively folded after SEC, as confirmed by cold sodium dodecyl sulfate polyacrylamide gel electrophoresis (SDS-PAGE; Figure 5c). While heat-denatured OmpLA migrated as expected for an unfolded polypeptide of 31 kg mol^{-1}, unboiled samples exhibited an apparent molar mass of 17 kg mol^{-1}, as previously shown for the native enzyme.[24]

Finally, we wondered whether DIBMA could extract integral membrane proteins from native membranes of *Escherichia coli*, the "workhorse" of heterologous protein
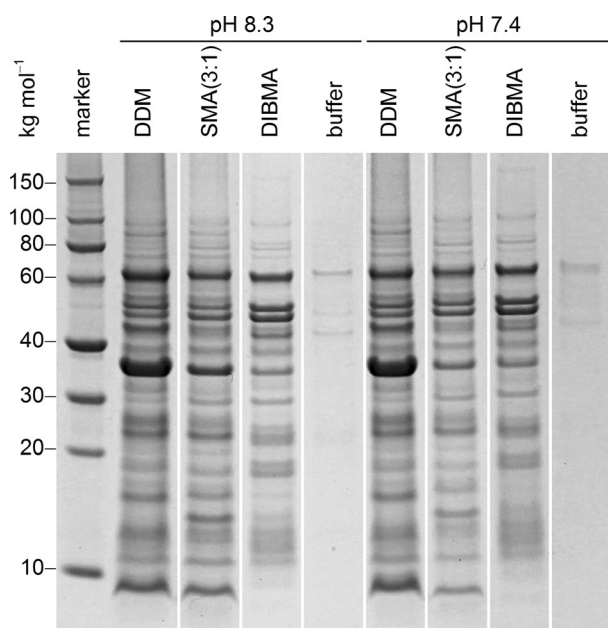
Figure 6. Solubilization of native *E. coli* BL21(DE3) membranes by 10 mM DDM, 2.5% (*w/v*) SMA(3:1), or 2.5% (*w/v*) DIBMA at 20°C as visualized by SDS-PAGE. Shown are the solubilized membrane-protein fractions after the removal of cell debris, intrinsically soluble proteins, and unsolubilized material by serial ultracentrifugation (see the Supporting Information).

production. In terms of solubilizing total membrane-protein mass, the efficiency of DIBMA relative to that of the gold-standard detergent *n*-dodecyl-β-ᴅ-maltopyranoside (DDM) amounted to around 70% at both pH values tested (Figure 6). For comparison, SMA(3:1) showed relative efficiencies of around 80% at pH 8.3 and 60% at pH 7.4. While DIBMA, SMA(3:1), and DDM solubilized various proteins to different extents, there were striking similarities among the overall SDS-PAGE patterns. Comparison with the total protein patterns of inner and outer *E. coli* membranes[27,28] indicates that DIBMA and SMA(3:1) can extract a wide range of membrane proteins from both bacterial membranes. Notably, polymer-mediated protein solubilization directly from the outer membrane has not otherwise been reported so far.[10]

In summary, we have demonstrated that DIBMA is a valuable addition to the small repertoire of amphiphilic polymers that are capable of extracting membrane proteins from cellular or model membranes to accommodate them in lipid-bilayer nanodiscs. DIBMALPs are chemically and thermally stable, have a narrow size distribution, and support the activity of an integral membrane enzyme. Unlike other nanodisc scaffolds, DIBMA has only a mild impact on lipid acyl-chain order, is compatible with far-UV spectroscopy without the prior removal of empty nanodiscs, and tolerates fairly high concentrations of divalent cations, which offers substantial advantages for in vitro studies on integral membrane proteins in a nanosized lipid-bilayer environment.

Conflict of interest

The authors declare no conflict of interest.

[1] J. P. Overington, B. Al-Lazikani, A. L. Hopkins, *Nat. Rev.* **2006**, *5*, 993–996.

[2] N. Bordag, S. Keller, *Chem. Phys. Lipids* **2010**, *163*, 1–26.

[3] T. H. Bayburt, S. G. Sligar, *FEBS Lett.* **2010**, *584*, 1721–1727.

[4] T. J. Knowles, R. Finka, C. Smith, Y. Lin, T. Dafforn, M. Overduin, *J. Am. Chem. Soc.* **2009**, *131*, 7484–7485.

[5] M. Orwick-Rydmark, J. E. Lovett, A. Graziadei, L. Lindholm, M. R. Hicks, A. Watts, *Nano Lett.* **2012**, *12*, 4687–4692.

[6] J. M. Dörr, M. C. Koorengevel, M. Schäfer, A. V. Prokofyev, S. Scheidelaar, W. van der Cruijsen, T. R. Dafforn, M. Baldus, J. A. Killian, *Proc. Natl. Acad. Sci. USA* **2014**, *111*, 18607–18612.

[7] S. Gulati, M. Jamshad, T. J. Knowles, K. A. Morrison, R. Downing, N. Cant, R. Collins, J. B. Koendrick, R. C. Ford, M. Overduin, I. Kerr, T. R. Dafforn, A. J. Rothnie, *Biochem. J.* **2014**, *461*, 269–278.

[8] D. J. K. Swainsbury, S. Scheidelaar, R. van Grondelle, J. A. Killian, M. R. Jones, *Angew. Chem. Int. Ed.* **2014**, *53*, 11803–11807; *Angew. Chem.* **2014**, *126*, 11997–12001.

[9] M. Jamshad, J. Charlton, Y. Lin, S. J. Routledge, Z. Bawa, T. J. Knowles, M. Overduin, N. Dekker, T. R. Dafforn, R. M. Bill, D. R. Poyner, M. Wheatley, *Biosci. Rep.* **2015**, *35*, e00188.

[10] J. M. Dörr, S. Scheidelaar, M. C. Koorengevel, J. J. Dominguez, M. Schäfer, C. A. van Walree, J. A. Killian, *Eur. Biophys. J.* **2016**, *45*, 3–21.

[11] S. C. Lee, T. J. Knowles, V. L. G. Postis, M. Jamshad, R. A. Parslow, Y. Lin, A. Goldman, P. Sridhar, M. Overduin, S. P. Muench, T. R. Dafforn, *Nat. Protoc.* **2016**, *11*, 1149–1162.

[12] C. Logez, M. Damian, C. Legros, C. Dupré, M. Guery, S. Mary, R. Wagner, C. M'Kadmi, O. Nosjean, B. Fould, J. Marie, J. Fehrentz, J. Martinez, G. Ferry, J. A. Boutin, J.-L. Banères, *Biochemistry* **2016**, *55*, 38–48.

[13] A. J. Rothnie, *Methods Mol. Biol.* **2016**, *1432*, 261–267.

[14] R. Cuevas Arenas, J. Klingler, C. Vargas, S. Keller, *Nanoscale* **2016**, *8*, 15016–15026.

[15] C. Vargas, R. Cuevas Arenas, E. Frotscher, S. Keller, *Nanoscale* **2015**, *7*, 20685–20696.

[16] P. T. Wong, *Annu. Rev. Biophys. Bioeng.* **1984**, *13*, 1–24.

[17] C. J. Orendorff, M. W. Ducey, J. E. Pemberton, *J. Phys. Chem. A* **2002**, *106*, 6991–6998.

[18] M. C. Orwick, P. J. Judge, J. Procek, L. Lindholm, A. Graziadei, A. Engel, G. Gröbner, A. Watts, *Angew. Chem. Int. Ed.* **2012**, *51*, 4653–4657; *Angew. Chem.* **2012**, *124*, 4731–4735.

[19] M. Jamshad, V. Grimard, I. Idini, T. J. Knowles, M. R. Dowle, N. Schofield, P. Sridhar, Y. Lin, R. Finka, M. Wheatley, O. R. T. Thomas, R. E. Palmer, M. Overduin, C. Govaerts, J. Ruysschaert, K. J. Edler, T. R. Dafforn, *Nano Res.* **2015**, *8*, 774–789.

[20] S. Scheidelaar, M. C. Koorengevel, J. D. Pardo, J. D. Meeldijk, E. Breukink, J. A. Killian, *Biophys. J.* **2015**, *108*, 279–290.

[21] J. A. Lundbæk, S. A. Collingwood, H. I. Ingólfsson, R. Kapoor, O. S. Andersen, *J. R. Soc. Interface* **2010**, *7*, 373–395.

[22] N. Dekker, K. Merck, J. Tommassen, H. M. Verheij, *Eur. J. Biochem.* **1995**, *232*, 214–219.

[23] C. P. Moon, S. Kwon, K. G. Fleming, *J. Mol. Biol.* **2011**, *413*, 484–494.

[24] S. Fiedler, L. Cole, S. Keller, *Anal. Chem.* **2013**, *85*, 1868–1872.

[25] J. Broecker, S. Keller, *Langmuir* **2013**, *29*, 8502–8510.

[26] D. Handa, H. Kimura, T. Oka, Y. Takechi, K. Okuhira, M. C. Phillips, H. Saito, *Biochemistry* **2015**, *54*, 1123–1131.

[27] K. Duquesne, J. N. Sturgis, *Methods Mol. Biol.* **2010**, *601*, 205–217.

[28] B. T. Arachea, Z. Sun, N. Potente, R. Malik, D. Isailovic, R. E. Viola, *Protein Expression Purif.* **2012**, *86*, 12–20.